MATERIALS SCIENCE

Functionalized lipid-like nanoparticles for in vivo mRNA delivery and base editing

Xinfu Zhang[1,2]*, Weiyu Zhao[1]*, Giang N. Nguyen[3], Chengxiang Zhang[1], Chunxi Zeng[1], Jingyue Yan[1], Shi Du[1], Xucheng Hou[1], Wenqing Li[1], Justin Jiang[1], Binbin Deng[4], David W. McComb[4,5], Robert Dorkin[6], Aalok Shah[6], Luis Barrera[6], Francine Gregoire[6], Manmohan Singh[6], Delai Chen[6†], Denise E. Sabatino[3,7†], Yizhou Dong[1,8,9,10,11,12†]

Messenger RNA (mRNA) therapeutics have been explored to treat various genetic disorders. Lipid-derived nanomaterials are currently one of the most promising biomaterials that mediate effective mRNA delivery. However, efficiency and safety of this nanomaterial-based mRNA delivery remains a challenge for clinical applications. Here, we constructed a series of lipid-like nanomaterials (LLNs), named functionalized TT derivatives (FTT), for mRNA-based therapeutic applications in vivo. After screenings on the materials, we identified FTT5 as a lead material for efficient delivery of long mRNAs, such as human factor VIII (hFVIII) mRNA (~4.5 kb) for expression of hFVIII protein in hemophilia A mice. Moreover, FTT5 LLNs demonstrated high percentage of base editing on PCSK9 in vivo at a low dose of base editor mRNA (~5.5 kb) and single guide RNA. Consequently, FTT nanomaterials merit further development for mRNA-based therapy.

INTRODUCTION

mRNA-based therapeutics hold great promise for the treatment of various types of diseases (*1*–*6*). For example, mRNA-mediated protein replacement therapy has been applied to treat several protein defective diseases in clinical trials (*2*, *7*). Through the intrinsic protein synthetic pathway, in vitro transcribed (IVT) mRNAs can supplement therapeutic proteins, such as intracellular, transmembrane, and secreted proteins, to restore the function of these essential proteins (*3*, *8*, *9*). In addition, recent advances in the delivery of Cas9 mRNA together with a single guide RNA (sgRNA) further expand the mRNA delivery to gene editing applications (*10*–*14*). By engineering the Cas9 protein, base editing has emerged to be a unique gene editing technology, which induces point mutations at the target site (*15*–*18*). Without a double-strand DNA break, base editing can lead to single nucleotide conversion and therefore can be used as a reliable tool for genome editing and potentially correct the disease-related mutations in the genome (*16*). In vivo mRNA delivery of base editors using lipid nanoparticles (LNPs) has attracted great interest (*19*, *20*), whereas most of the current studies used viral vectors for in vivo base editing or direct gene engineering on zygotes (*16*, *21*).

As mRNA molecules are vulnerable to ribonuclease enzymes that widely exist in the biological systems and highly negatively charged, which compromise their internalization through cell membranes, suitable in vivo mRNA delivery systems are urgently needed (*4*). To protect and deliver mRNA, extensive efforts have been devoted to construct biocompatible carriers, such as LNPs, polymeric nanoparticles, peptides/protein-mRNA complexes, and other types of biomaterials (*9*, *22*, *23*). Among these reported platforms, lipid-like nanoparticles (LLNs) are one of the representative materials that have been extensively used for mRNAs delivery in vivo. Early-stage mRNA delivery LNPs mainly involve cationic lipids, such as DOTAP and DOTMA (*6*, *9*). Later on, researchers spent substantial efforts on developing ionizable lipid derivatives to maximize the efficiency and maintain low toxicity in vivo (*6*, *24*–*27*). A few recently reported LLNs, such as TT3, 5A2-SC8, and A18-Iso5-2 DC18, have shown efficient delivery and therapeutic applications of mRNA in disease models (*28*–*32*). In addition, several lipid-based nanoparticles, such as LP-01, TT3, and cKK-E12, have been reported as the delivery system of Cas9 mRNA and sgRNA for gene editing applications (*6*, *33*, *34*). These promising results in preclinical studies encourage us to further explore new LLNs and their therapeutic potential.

We previously reported a library of lipid-like compounds, N^1,N^3,N^5-tris(2-aminoethyl)benzene-1,3,5-tricarboxamide (TT) derivatives, which comprise a phenyl core and six alkyl lipid chains (*28*). In particular, TT3 LLNs effectively delivered human factor IX (hFIX) mRNA for hemophilia B therapy and induced gene editing on PCSK9 in different animal models (*28*, *34*). Here, to promote in vivo mRNA delivery with tunable biodegradability of nanomaterials, we designed a series of functionalized TT (FTT) LLNs by combining the core structure of TT3 with different types of biodegradable lipid chains. We screened their delivery efficiency through both in vitro and in vivo assays and identified a top-performing material, FTT5 LLNs. Furthermore, FTT5 LLNs were evaluated for the in vivo mRNA delivery capability and base editing applications.

RESULTS

Synthesis and formulation of FTT materials

First, we synthesized a set of lipid-like compounds through a one-step reductive amination of the core structure with various lipid

[1]Division of Pharmaceutics and Pharmacology, College of Pharmacy, The Ohio State University, Columbus, OH 43210, USA. [2]State Key Laboratory of Fine Chemicals, Dalian University of Technology, Dalian 116024, China. [3]The Children's Hospital of Philadelphia, Philadelphia, PA 19104, USA. [4]Center for Electron Microscopy and Analysis, Department of Materials Science and Engineering, The Ohio State University, Columbus, OH 43210, USA. [5]Department of Materials Science and Engineering, The Ohio State University, Columbus, OH 43210, USA. [6]Beam Therapeutics, Cambridge, MA 02139, USA. [7]Perelman School of Medicine, University of Pennsylvania, Philadelphia, PA 19104, USA. [8]Department of Biomedical Engineering, The Ohio State University, Columbus, OH 43210, USA. [9]The Center for Clinical and Translational Science, The Ohio State University, Columbus, OH 43210, USA. [10]The Comprehensive Cancer Center, The Ohio State University, Columbus, OH 43210, USA. [11]Dorothy M. Davis Heart and Lung Research Institute, The Ohio State University, Columbus, OH 43210, USA. [12]Department of Radiation Oncology, The Ohio State University, Columbus, OH 43210, USA.
*These authors contributed equally to this work.
†Corresponding author. Email: dong.525@osu.edu (Y.D.); dsabatin@pennmedicine.upenn.edu (D.E.S.); dchen@beamtx.com (D.C.)

aldehydes. As shown in Fig. 1A, these newly synthesized materials can be classified into three categories based on the structure of their lipid chains: carbon chains, branched ester chains, and linear ester chains. These lipid-like compounds share the same core structure as TT3. Therefore, we named this series of materials as FTT derivatives. FTT1 is equipped with an unsaturated hydrocarbon chain; FTT2 to FTT6 are installed with different branched esters; FTT7 to FTT10 are incorporated with different linear esters with less steric effects than FTT2 to FTT6. We validated the chemical structures of FTT1 to FTT10 using proton nuclear magnetic resonance and mass spectrum.

Newly synthesized FTT compounds were then formulated into FTT LLN formulations, according to previously reported methods (*28*). Formulation components include FTT lipids, 1,2-dioleoyl-sn-glycero-3-phosphoethanolamine (DOPE), cholesterol, 1,2-dimyristoyl-rac-glycero-3-methoxypolyethylene glycol-2000 (DMG-PEG_{2000}), and firefly luciferase mRNA (FLuc mRNA). The molar ratio of components within FTT LLN formulations was 20/30/40/0.75 (FTT lipids/DOPE/cholesterol/DMG-PEG_{2000}) (*28*). To prepare the formulations, mRNA molecules were dissolved in aqueous phase, while other components were dissolved in ethanol phase. Through rapid mixing of ethanol and aqueous phases by either mechanical pipetting or a microfluidic device, FTT LLN formulations were afforded.

Screening of FTT1-10 LLNs for mRNA delivery

Then, we investigated the mRNA delivery capability of FTT1-10 LLNs encapsulating FLuc mRNA in the hepatocellular carcinoma Hep3B cell line. We treated Hep3B cells with freshly prepared LLNs at 50 ng per well FLuc mRNA concentration in 96-well plates. As shown in fig. S1A, most of these FTT LLNs showed a comparable firefly luciferase expression level as TT3 LLNs. These results encouraged us to further perform the in vivo studies. The sizes of FTT1-10 LLNs for in vivo screenings were from 88 to 107 nm with polydispersity index (PDI) lower than 0.3 (Fig. 1B). We intravenously injected FLuc mRNA–encapsulated FTT LLNs (0.5 mg/kg) in mice using TT3 LLNs as a reference. We quantified the bioluminescence intensity from major organs, 6 hours after administration. As shown in fig. S2, among the FTT LLNs, FTT5 LLN–treated mice showed significantly higher bioluminescence intensity in different organs as compared to TT3 LLNs. FTT5 LLN–treated group increased the luciferase expression efficiency of TT3 LLNs for around twofold in the liver (Fig. 1C and fig. S3), which indicated that FTT5 LLNs displayed a favorable property for mRNA delivery in the liver. Therefore, we selected FTT5 LLNs as a lead material for further characterizations and explorations on their therapeutic applications with liver as the target organ.

Characterization of FTT5 LLNs

We conducted additional studies aiming at optimizing the formulation of FTT5 LLNs through an orthogonal array design–based experiments. As shown in figs. S4 and S5, we adjusted the molar ratio of the formulation components in FTT5 LLNs and replaced several components, such as DOPE and DMG-PEG_{2000}, with different lipid

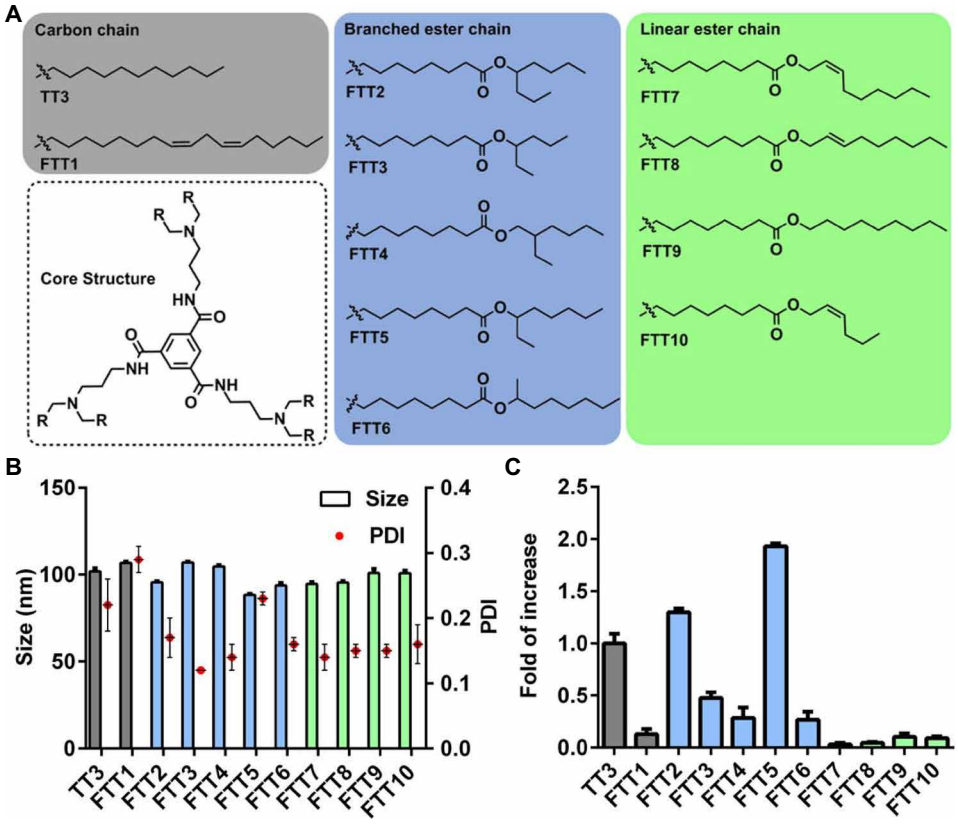

Fig. 1. Design and screenings of FTT LLNs. (**A**) Chemical structures of the FTT derivatives. FTT1 to FTT10 compounds share the same core structure and have three different types of lipid side chains, which are presented as gray (carbon chain), blue (branched ester chain), and green (linear ester chain), respectively. (**B**) Size and polydispersity index (PDI) of FLuc mRNA–encapsulated FTT1 to FTT10 LLNs for in vivo screenings. (**C**) In vivo mRNA delivery efficiency of FTT1 to FTT10 LLNs, represented as fold of increase in the luminescence intensity of FTT LLNs to that of TT3 LLNs in the livers of mice ($n = 2$).

materials. Several LLNs in the orthogonal experiments showed higher in vitro efficiency than the original FTT5 LLNs (figs. S4 and S5). However, these optimized LLNs showed lower in vivo efficiency as compared to the original formulation (figs. S4G and S5H). Thus, we chose the original formulation of FTT5 LLNs and further characterized the FTT5 LLNs on their physicochemical properties, biodegradability, and potential mechanism of internalization. The particle size of FTT5 LLNs was around 100 nm according to the measurements by dynamic light scattering (DLS), with PDI lower than 0.2 (Fig. 2A). Images of FTT5 LLNs captured by cryo–transmission electron microscopy (cryo-TEM) displayed that FTT5 LLNs had spherical structures with size around 100 nm, which was consistent with the DLS measurements (Fig. 2C and fig. S6). In addition, FTT5 LLNs showed slightly negative charge around −11 mV and an encapsulation of around 91% of mRNAs (Fig. 2B). We then evaluated the in vivo biodegradability of FTT5 and FTT9 LLNs, which are the representatives from the branched and linear ester chain groups, respectively. After FTT5 and FTT9 LLNs were systemically administered, the remaining levels of two lipids in the liver and blood of mice were determined by mass spectrometry at different time points. As shown in Fig. 2 (D and E), both FTT5 and FTT9 LLNs showed fast clearance from blood. Both LLNs reached the peak level in the liver right after the administration. FTT9 was cleared more than 80% in the first 6 hours after administration and complete clearance in 24 hours; whereas FTT5 showed slower clearance from the liver and up to 50% clearance in 48 hours. These

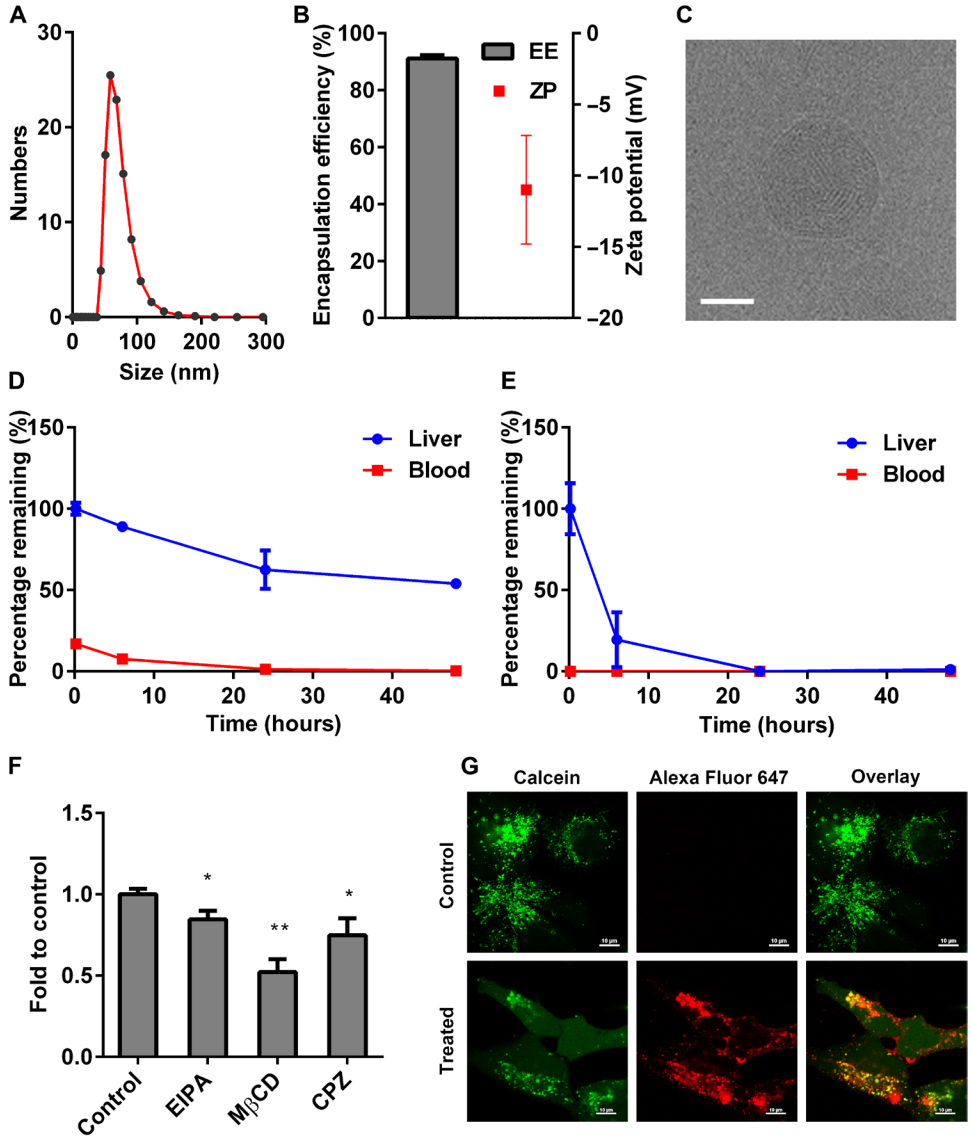

Fig. 2. Characterization of FTT5 LLNs. (**A**) Size distribution of FTT5 LLNs measured by DLS. (**B**) mRNA encapsulation efficiency (EE) and zeta potential (ZP) of FTT5 LLNs. (**C**) Cryo-TEM image of an FTT5 LLN. Scale bar, 50 nm. (**D** and **E**) Biodegradation of FTT5 and FTT9 LLNs in the liver and blood of mice within 48 hours, respectively ($n = 3$). (**F**) Fold of changes in the cellular uptake of FTT5 LLNs with the treatment of different endocytic inhibitors, EIPA, MβCD, and CPZ, as compared with control group ($n = 3$; two-tailed Student's t test; $^*P < 0.05$; $^{**}P < 0.01$). (**G**) Confocal microscopy images on the endosomal escape of FTT5 LLNs. Diffusion of calcein was observed in the cytosol of cells in the presence of FTT5 LLNs containing Alexa Fluor 647–labeled RNA, suggesting that FTT5 LLNs mediated a rupture of endosomal membranes and thus led to a release of the RNAs from endosomes. Scale bars, 10 μm.

results validated that ester chains with different steric effects could regulate the degradation rate of FTT materials. Further study on the internalization mechanism of FTT5 LLNs showed that endocytic inhibitors, 5-(*N*-Ethyl-*N*-isopropyl)amiloride (EIPA), methyl-β-cyclodextrin (MβCD), and chlorpromazine (CPZ) inhibited the cellular uptake of FTT5 LLNs for about 15, 48, and 25%, respectively, indicating that the cellular uptake of FTT5 LLNs involved multiple endocytic pathways (Fig. 2F). In addition, the calcein assay indicated that the endosomal escape of FTT5 LLNs was through the rupture of endosomal membranes (Fig. 2G).

FTT5 LLNs for hFVIII mRNA delivery and base editing in vivo

Hemophilia is a type of genetic disease that has impaired blood clotting ability (*35*). Prophylactic protein replacement treatments are needed for hemophilia patients to prevent spontaneous bleedings (*35*, *36*). Hemophilia A, due to a deficiency in the coagulation protein FVIII, is the most common type of hemophilia (*37*). As a proof-of-concept study, we investigated the delivery of hFVIII mRNA in vivo using FTT5 LLNs for hemophilia A treatment. We performed in vivo administration of FTT5-hFVIII mRNA LLNs in wild-type (WT) mice and hemophilia A mice. We measured the circulating protein level of hFVIII in WT mice by enzyme-linked immunosorbent assay (ELISA) that detects hFVIII but not murine FVIII at 6 and 12 hours after intravenous injection of FTT5-hFVIII mRNA LLNs (2 mg/kg) (*36*, *37*). Treated mice produced more than 140 ng/ml hFVIII at both time points, achieving hFVIII protein levels within the normal clinical range (100 to 200 ng/ml), which demonstrated potent therapeutic mRNA delivery and protein expression (Fig. 3A). We then further applied the formulation to hemophilia A mice that have no detectable FVIII protein or activity at the same mRNA dose. Consistently, FTT5 LLNs induced significant production of hFVIII more than 220 ng/ml at both 6 and 12 hours after administration based on ELISA assay (Fig. 3B). Coatest assay further showed that the activity of hFVIII was 73% at 6 hours and reached to 90% at 12 hours after administration (Fig. 3C). Therefore, hFVIII mRNA–encapsulated FTT5 LLNs was able to restore the hFVIII level up to 90% of normal activity. On the basis of results from the histology study in the hemophilia A mice, no specific pathological changes were present in examined tissues after treatment (Fig. 3D).

To further explore the in vivo application of LLNs, we investigated them for base editing. We coencapsulated an mRNA encoding adenine base editor (~5.5 kb) and an sgRNA targeting PCSK9 at the mass ratio of 1:1 into TT3 and FTT5 LLNs, respectively. The afforded TT3 and FTT5 LLNs were administered to mice via tail vein injections. In vivo base editing (A to G mutation) efficiency in liver was determined by targeted deep sequencing analysis on DNA extracted from the liver biopsy. We evaluated the base editing efficiency of TT3 LLNs at two different dose levels (0.15 and 1.5 mg/kg). Results showed that TT3 LLNs mediated more than 40% of base editing efficiency (% A to G mutation) and a marked reduction of the serum PCSK9 protein level (fig. S7, A and B). Then, we compared the editing efficiency between TT3 and FTT5 LLNs and found that FTT5 LLNs further enhanced the editing efficiency of TT3 LLNs by 1.32-fold (fig. S7C). Last, we studied the dose response of FTT5 LLNs for the in vivo base editing of the PCSK9 gene. The editing efficiency (% A to G mutation) plateaued at ~60% at 1 mg/kg of total RNA dose, presumably due to the presence of nonhepatic cells that are less prone to LLN delivery in the liver tissue. Notably, the dose-response suggests a median effective concentration of <0.125 mg/kg, a potency that is unmatched in previous reports of in vivo base editing (Fig. 4, A and B).

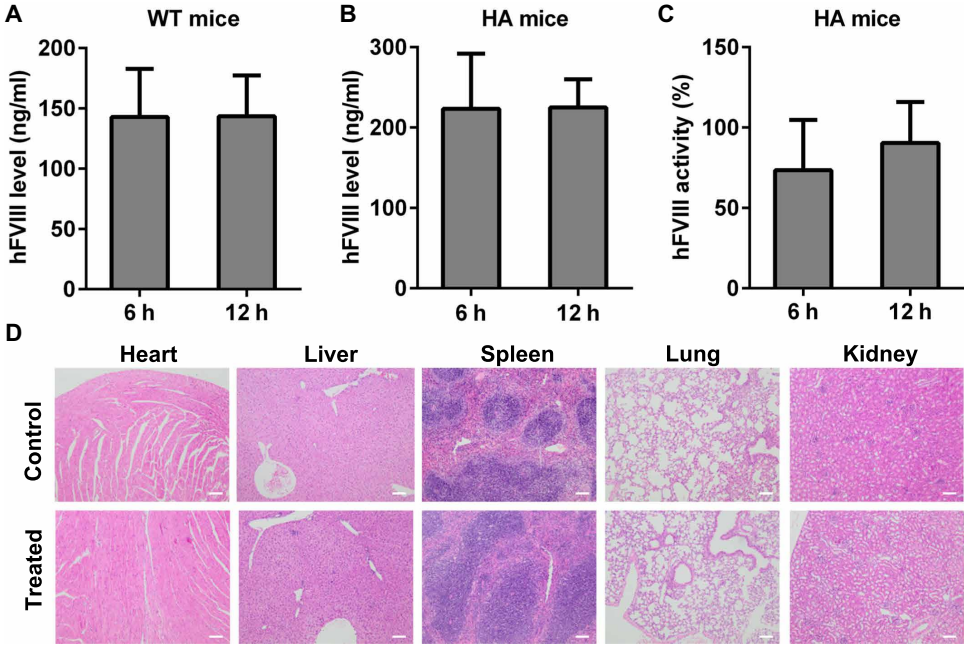

Fig. 3. In vivo hFVIII mRNA delivery using FTT5-LLNs. (**A**) hFVIII protein level in WT mice 6 and 12 hours after intravenous administration of FTT5-hFVIII mRNA LLNs at an mRNA dose of 2 mg/kg ($n = 3$). (**B**) hFVIII protein level and (**C**) activity in hemophilia A (HA) mice 6 and 12 hours after intravenous administration of FTT5-hFVIII mRNA LLNs at an mRNA dose of 2 mg/kg ($n = 3$). (**D**) Histopathological images from hemophilia A mice treated with FTT5-hFVIII mRNA LLNs and untreated hemophilia A mice as a control. Scale bars, 100 μm.

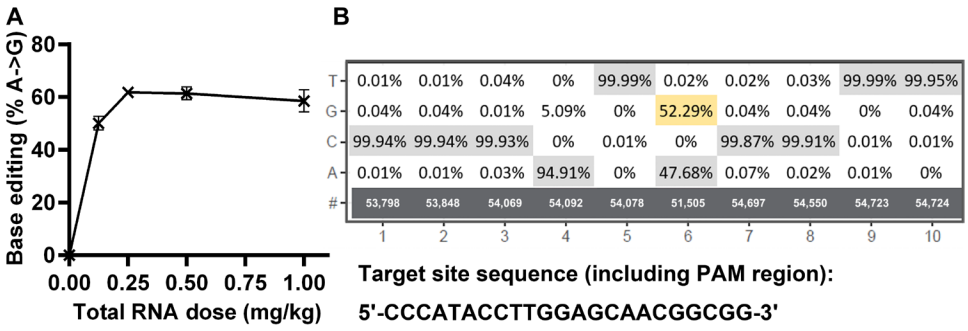

Fig. 4. In vivo base editing of PCSK9 gene using FTT5 LLNs. (**A**) In vivo dose-response curve of base editing of the PCSK9 gene ($n = 5$). (**B**) Representative targeted deep sequencing data from a mouse treated at a dose of 0.125 mg/kg.

DISCUSSION

In summary, we synthesized and screened a series of lipid-like nanomaterials by chemically optimizing our previously reported material, TT3, with various ester tails, to enable tunable biodegradability in vivo. We examined delivery efficiency of these materials and compared them with TT3 LLNs. On the basis of the screening results from in vivo luciferase assay, we found that lipid-like nanomaterials with branched ester chains (FTT2 to FTT6) mainly delivered mRNAs into liver and spleen, with a generally higher delivery efficiency as compared to the LLNs with linear ester chains (FTT7 to FTT10). In addition, the branch position and length within the branched ester structure of FTT could further affect the mRNA delivery in individual organs. Among all the FTT LLNs, FTT5 LLNs displayed the highest delivery efficiency to the liver, about twofold of TT3 LLNs. Further characterizations showed that FTT5 LLNs are in spherical morphology and are capable of mediating endosomal escape. In addition, biodegradability studies on FTT5 LLNs indicated that branched ester side chains mediate a slower degradation rate in the liver as compared to the FTT9 with linear ester chain, which might further lead to the differences in the delivery and expression of the payload mRNA molecules.

To explore the therapeutic potential of FTT5 LLNs in vivo, we applied FTT5 LLNs for the delivery of two long mRNA molecules: hFVIII mRNA (~4.5 k nucleotides) and adenine base editor mRNA (~5.5 k nucleotides). FTT5 LLNs showed efficient delivery of FVIII mRNA and potent expression of hFVIII protein in both WT mice and hemophilia A mice and restored the hFVIII level to normal at the dose of 2 mg/kg. In addition, FTT5 LLNs also demonstrated potent base editing capability in vivo at low doses. Toxicity study based on observation and histopathology analysis revealed that FTT5 LLNs were well tolerated in mice at the therapeutic dose tested in this study.

As a conclusion, our chemical design of new lipid-like nanomaterials further improved the delivery efficiency of TT3 and demonstrated its promise for versatile mRNA-based gene therapies. Overall, the lead FTT5 LLNs merit future preclinical and potential clinical evaluation.

MATERIALS AND METHODS

Experimental design

A series of FTT LLNs were designed by combining the core structure of TT with various types of biodegradable lipid chains to improve in vivo mRNA delivery with tunable biodegradability of nanomaterials. Experimental details for the synthesis of FTT lipids are included in the Supplementary Materials.

Materials and reagents

DOPE, DMG-PEG$_{2000}$, and C18-CONH-PEG$_{2000}$ and other lipid materials were acquired from Avanti Polar Lipids Inc. (Alabaster, AL). Eagle's minimum essential medium (EMEM) and other cell culture supplies were purchased from Corning Incorporated (Corning, NY). Quant-iT RiboGreen RNA reagent and Gibco heat-inactivated fetal bovine serum (FBS) were acquired from Thermo Fisher Scientific (Waltham, MA). All the other chemical reagents were obtained from Sigma-Aldrich or Alfa Aesar and used without further purifications.

mRNAs were synthesized through IVT using the AmpliScribe T7-Flash Transcription Kit (Lucigen Corporation, Middleton, WI) and followed by the addition of a Cap1 structure using the Vaccinia Capping System and mRNA Cap 2′-*O*-methyltransferase (New England Biolabs, Ipswich, MA). Pseudouridine-5′-triphosphate (TriLink BioTechnologies, San Diego, CA) was used for synthesizing ψ modified mRNA. mRNAs were purified through RNA Clean & Concentrator Kits (Zymo Research, Irvine, CA) before diluted in Tris-EDTA (TE) buffer for applications.

Preparation and characterizations of FTT1 to FTT10 LLNs

FTT1 to FTT10 LLN formulations were formulated following the previously reported TT3 LLN formulation (*28*). The molar ratio of FTT, DOPE, cholesterol, and DMG-PEG$_{2000}$ was 20:30:40:0.75. Briefly, in the ethanol phase, we mixed each FTT lipid with other helper lipids at the aforesaid molar ratio (*28*). FLuc mRNA was first diluted in citrate acid buffer and then mixed with the ethanol phase. Pipetting technique was used for preparing the formulations for in vitro studies, and the NanoAssemblr benchtop microfluidic device from Precision NanoSystems (Vancouver, BC, Canada) was used for formulations used in cryo-TEM and in vivo studies.

To characterize the physicochemical properties of LLNs, DLS measurement was adopted. We measured the particle size, PDI, and zeta potential of FTT1 to FTT10 LLNs by using Nano ZS Zetasizer (Malvern, Worcestershire, U.K.). In addition, we determined the mRNA encapsulation efficiency of FTT1 to FTT10 LLNs via a RiboGreen assay (*28*).

In vitro screening using luciferase assay

Hep3B cells were maintained and subcultured in 10% FBS containing EMEM. For in vitro luciferase assay, 2×10^4 cells per well of

Hep3B cells were seeded 1 day before the treatment in white-bottom 96-well plates. Then, cells were incubated with FLuc mRNA-FTT LLNs (50 ng mRNA per well, in triplicate). We measured the luminescence intensity of each well with the SpectraMax M5 microplate reader (Molecular Devices LLC., Sunnyvale, CA).

In vivo screening using IVIS imaging

All mouse experiments were performed under the protocols approved by the Institutional Animal Care and Use Committee and also complied with all relevant ethical regulations as applicable. C57BL/6 mice were injected intravenously with FTT1 to FTT10 LLNs or TT3 LLNs (mRNA dose of 0.5 mg/kg, two mice in each group). Six hours after intravenous injection, 150 μl per mouse of XenoLight D-luciferin (30 mg/ml; PerkinElmer, Waltham, MA) was injected to each mouse through intraperitoneal injection. Eight minutes after the injection of substrate, mice were euthanized. Also, major organs (heart, liver, spleen, lung, and kidneys) were collected, weighed, and imaged under Xenogen in vivo imaging system (IVIS; Caliper, Alameda, CA). Total flux (photons/sec) of bioluminescence in each organ was quantified and normalized by the organ weight.

Characterizations on the physiochemical properties of FTT5 LLNs

Physicochemical properties of FTT5 LLNs were determined using the aforesaid methods. Cryo-TEM imaging of FTT5 LLNs were carried out by Tecnai F20 S/TEM (FEI, Hillsboro, OR). In addition, cryo-TEM images were captured using a Gatan UltraScan 4K charge-coupled device camera with the specimen temperature maintained lower than 170°C under low-dose conditions.

Cellular uptake and endosomal escape of FTT5 LLNs

For endocytic pathways study, 2×10^4 cells per well of Hep 3B cells were seeded in 24-well plates and allowed to attach to the bottom of plates for overnight. Then, a cellular uptake assay was carried out by treating cells with enhanced green fluorescent protein mRNA-encapsulated FTT5 LLNs with the addition of different endocytic inhibitors, EIPA, MβCD, and CPZ, respectively. We used BD LSR II flow cytometry analyzer (BD Biosciences, San Jose, CA) for quantifying the cellular uptake of cells in the presence of different inhibitors. For the endosomal escape assay, 2×10^4 cells per well of Hep 3B cells were seeded in an ibidi μ-Dish 35-mm Quad dish (ibidi GmbH, Gräfelfing, Germany) and incubated overnight. Then, cells were treated with Alexa Fluor 647–labeled RNA containing FTT5 LLNs for 6 hours followed by the addition of calcein (150 μg/ml) in each well as previously reported (*38*). After washing with phosphate-buffered saline, images of cells were captured by a Nikon A1R Live Cell Imaging Confocal Microscope (Melville, NY) and analyzed by NIS-Elements.

In vivo biodegradation of FTT5 and FTT9 LLNs

The prepared FTT5 or FTT9 LLNs were intravenously injected at an mRNA dose of 1.8 mg/kg. The blood and liver were collected and analyzed at 20 min, 6, 24, or 48 hours after injection. Briefly, 50-μl aliquot of blood was immediately added to 1 ml of methanol in 1.5-ml Eppendorf tubes and mixed well by shaking. Liver was collected and immediately frozen by liquid nitrogen. Fifty-milligram aliquot of liver was transferred to 1 ml of methanol in 1.5-ml Eppendorf tubes and mixed well by vortex. To measure the samples using mass spectrometry, 0.5 ml of CH_2Cl_2 was added into each sample and followed by shaking vigorously for 5 min. The afforded solutions were measured by LTQ Orbitrap mass spectrometry (Thermo Fisher Scientific, Waltham, MA) after filtration.

In vivo hFVIII mRNA delivery and base editing

C57BL/6 mice were injected intravenously with FVIII-CO3 (ψ) mRNA–encapsulated FTT5 LLNs at the dose of 2 mg/kg. Six or twelve hours after intravenous injection, blood was collected from mice through cardiac puncture. We immediately mixed the blood samples with 3.8% sodium citrate buffer by inverting several times after blood collection and spun at 4°C at 7500 × *g* for 10 min. After centrifugation, plasma was collected, and hFVIII antigen levels were determined by ELISA assay, which does not cross-react with murine FVIII (*39*). The normal range of hFVIII in humans is 100 to 200 ng/ml (*40*). The standard for the ELISA was recombinant hFVIII (Xyntha, Pfizer) with 100% defined as 150 ng/ml. The same protocol was used for C57BL6/129 hemophilia A mice that have no detectable FVIII antigen or activity. In addition, Coatest SP4 FVIII (Chromogenix, Milan, Italy) was used to evaluate the FVIII activity after treatment (*39*). The standard for the Coatest was recombinant hFVIII (Xyntha, Pfizer) with 1 IU/ml defined as 100%.

For base editing, mRNA encoding adenine base editor and a sgRNA targeting mouse PCSK9 at 1:1 (mass ratio) were coencapsulated in FTT5 LLNs. The LLNs were administrated into Balb/c mice through tail vein injections at indicated total RNA doses. At 7 days after dosing, mice were euthanized and liver biopsy was harvested. Base editing was determined by performing targeted deep sequencing analysis at the PCSK9 target site using DNA extracted from the liver biopsy. The serum PCSK9 protein level in mice was quantified using an ELISA assay.

Histology study

FVIII-CO3 (ψ) mRNA–encapsulated FTT5 LLNs were injected intravenously into hemophilia A mice at the dose of 2 mg/kg. After 72 hours of treatment, mice were euthanized to collect organs for histological studies. Organs were soaked in 4% formaldehyde overnight and then switched into 75% ethanol for storage. To carry out the histological analysis, tissues were embedded into paraffin, sectioned, hematoxylin and eosin–stained, and imaged under microscope. Untreated mice were used as control. The histological analysis was performed by a professional pathologist of the Comparative Pathology and Mouse Phenotyping Shared Resource (CPMPSR) at The Ohio State University.

Statistical analysis

Data were statistically analyzed using GraphPad Prism or Excel. Samples were tested in triplicates for in vitro studies, and data were showed as means ± SD. Student's *t* test was used to determine the statistical significance. Sample sizes (*n*) for in vivo studies were annotated in figure legends.

SUPPLEMENTARY MATERIALS

Supplementary material for this article is available at http://advances.sciencemag.org/cgi/content/full/6/34/eabc2315/DC1

View/request a protocol for this paper from *Bio-protocol*.

REFERENCES AND NOTES

1. K. A. Hajj, K. A. Whitehead, Tools for translation: Non-viral materials for therapeutic mRNA delivery. *Nat. Rev. Mater.* **2**, 17056 (2017).

2. U. Sahin, K. Karikó, Ö. Türeci, mRNA-based therapeutics—developing a new class of drugs. *Nat. Rev. Drug Discov.* **13**, 759–780 (2014).
3. Q. Xiong, G. Y. Lee, J. Ding, W. Li, J. Shi, Biomedical applications of mRNA nanomedicine. *Nano Res.* **11**, 5281–5309 (2018).
4. N. Pardi, M. J. Hogan, F. W. Porter, D. Weissman, mRNA vaccines – a new era in vaccinology. *Nat. Rev. Drug Discov.* **17**, 261–279 (2018).
5. S. Patel, A. Athirasala, P. P. Menezes, N. Ashwanikumar, T. Zou, G. Sahay, L. E. Bertassoni, Messenger RNA delivery for tissue engineering and regenerative medicine applications. *Tissue Eng. Part A* **25**, 91–112 (2019).
6. P. S. Kowalski, A. Rudra, L. Miao, D. G. Anderson, Delivering the messenger: Advances in technologies for therapeutic mRNA delivery. *Mol. Ther.* **27**, 710–728 (2019).
7. W. Zhao, X. Hou, O. G. Vick, Y. Dong, RNA delivery biomaterials for the treatment of genetic and rare diseases. *Biomaterials* **217**, 119291 (2019).
8. M. A. Islam, E. K. G. Reesor, Y. Xu, H. R. Zope, B. R. Zetter, J. Shi, Biomaterials for mRNA delivery. *Biomater. Sci.* **3**, 1519–1533 (2015).
9. B. Li, X. Zhang, Y. Dong, Nanoscale platforms for messenger RNA delivery. *Wiley Interdiscip. Rev. Nanomed. Nanobiotechnol.* **11**, e1530 (2019).
10. H.-X. Wang, M. Li, C. M. Lee, S. Chakraborty, H.-W. Kim, G. Bao, K. W. Leong, CRISPR/Cas9-based genome editing for disease modeling and therapy: Challenges and opportunities for nonviral delivery. *Chem. Rev.* **117**, 9874–9906 (2017).
11. L. Li, S. Hu, X. Chen, Non-viral delivery systems for CRISPR/Cas9-based genome editing: Challenges and opportunities. *Biomaterials* **171**, 207–218 (2018).
12. C. Liu, L. Zhang, H. Liu, K. Cheng, Delivery strategies of the CRISPR-Cas9 gene-editing system for therapeutic applications. *J. Control. Release* **266**, 17–26 (2017).
13. J. B. Miller, D. J. Siegwart, Design of synthetic materials for intracellular delivery of RNAs: From siRNA-mediated gene silencing to CRISPR/Cas gene editing. *Nano Res.* **11**, 5310–5337 (2018).
14. J. Liu, J. Chang, Y. Jiang, X. Meng, T. Sun, L. Mao, Q. Xu, M. Wang, Fast and efficient CRISPR/Cas9 genome editing in vivo enabled by bioreducible lipid and messenger RNA nanoparticles. *Adv. Mater.* **31**, e1902575 (2019).
15. Y. B. Kim, A. C. Komor, J. M. Levy, M. S. Packer, K. T. Zhao, D. R. Liu, Increasing the genome-targeting scope and precision of base editing with engineered Cas9-cytidine deaminase fusions. *Nat. Biotechnol.* **35**, 371–376 (2017).
16. H. A. Rees, D. R. Liu, Base editing: Precision chemistry on the genome and transcriptome of living cells. *Nat. Rev. Genet.* **19**, 770–788 (2018).
17. A. C. Rossidis, J. D. Stratigis, A. C. Chadwick, H. A. Hartman, N. J. Ahn, H. Li, K. Singh, B. E. Coons, L. Li, W. Lv, P. W. Zoltick, D. Alapati, W. Zacharias, R. Jain, E. E. Morrisey, K. Musunuru, W. H. Peranteau, In utero CRISPR-mediated therapeutic editing of metabolic genes. *Nat. Med.* **24**, 1513–1518 (2018).
18. N. M. Gaudelli, A. C. Komor, H. A. Rees, M. S. Packer, A. H. Badran, D. I. Bryson, D. R. Liu, Programmable base editing of A•T to G•C in genomic DNA without DNA cleavage. *Nature* **551**, 464–471 (2017).
19. T. Jiang, J. M. Henderson, K. Coote, Y. Cheng, H. C. Valley, X.-O. Zhang, Q. Wang, L. H. Rhym, Y. Cao, G. A. Newby, H. Bihler, M. Mense, Z. Weng, D. G. Anderson, A. P. McCaffrey, D. R. Liu, W. Xue, Chemical modifications of adenine base editor mRNA and guide RNA expand its application scope. *Nat. Commun.* **11**, 1979 (2020).
20. C.-Q. Song, T. Jiang, M. Richter, L. H. Rhym, L. W. Koblan, M. P. Zafra, E. M. Schatoff, J. L. Doman, Y. Cao, L. E. Dow, L. J. Zhu, D. G. Anderson, D. R. Liu, H. Yin, W. Xue, Adenine base editing in an adult mouse model of tyrosinaemia. *Nat. Biomed. Eng.* **4**, 125–130 (2020).
21. J. M. Levy, W.-H. Yeh, N. Pendse, J. R. Davis, E. Hennessey, R. Butcher, L. W. Koblan, J. Comander, Q. Liu, D. R. Liu, Cytosine and adenine base editing of the brain, liver, retina, heart and skeletal muscle of mice via adeno-associated viruses. *Nat. Biomed. Eng.* **4**, 97–110 (2020).
22. M. P. Lokugamage, Z. Gan, C. Zurla, J. Levin, F. Z. Islam, S. Kalathoor, M. Sato, C. D. Sago, P. J. Santangelo, J. E. Dahlman, Mild innate immune activation overrides efficient nanoparticle-mediated RNA delivery. *Adv. Mater.* **32**, e1904905 (2020).
23. M. M. Billingsley, N. Singh, P. Ravikumar, R. Zhang, C. H. June, M. J. Mitchell, Ionizable lipid nanoparticle-mediated mRNA delivery for human CAR T cell engineering. *Nano Lett.* **20**, 1578–1589 (2020).
24. O. S. Fenton, K. J. Kauffman, R. L. McClellan, E. A. Appel, J. R. Dorkin, M. W. Tibbitt, M. W. Heartlein, F. DeRosa, R. Langer, D. G. Anderson, Bioinspired alkenyl amino alcohol ionizable lipid materials for highly potent in vivo mRNA delivery. *Adv. Mater.* **28**, 2939–2943 (2016).
25. K. J. Kauffman, J. R. Dorkin, J. H. Yang, M. W. Heartlein, F. DeRosa, F. F. Mir, O. S. Fenton, D. G. Anderson, Optimization of lipid nanoparticle formulations for mRNA delivery in vivo with fractional factorial and definitive screening designs. *Nano Lett.* **15**, 7300–7306 (2015).
26. P. Midoux, C. Pichon, Lipid-based mRNA vaccine delivery systems. *Expert Rev. Vaccines* **14**, 221–234 (2015).
27. O. S. Fenton, K. J. Kauffman, J. C. Kaczmarek, R. L. McClellan, S. Jhunjhunwala, M. W. Tibbitt, M. D. Zeng, E. A. Appel, J. R. Dorkin, F. F. Mir, J. H. Yang, M. A. Oberli, M. W. Heartlein, F. DeRosa, R. Langer, D. G. Anderson, Synthesis and biological evaluation of ionizable lipid materials for the in vivo delivery of messenger RNA to B lymphocytes. *Adv. Mater.* **29**, 1606944 (2017).
28. B. Li, X. Luo, B. Deng, J. Wang, D. W. McComb, Y. Shi, K. M. L. Gaensler, X. Tan, A. L. Dunn, B. A. Kerlin, Y. Dong, An orthogonal array optimization of lipid-like nanoparticles for mRNA delivery in vivo. *Nano Lett.* **15**, 8099–8107 (2015).
29. E. Robinson, K. D. MacDonald, K. Slaughter, M. McKinney, S. Patel, C. Sun, G. Sahay, Lipid nanoparticle-delivered chemically modified mRNA restores chloride secretion in cystic fibrosis. *Mol. Ther.* **26**, 2034–2046 (2018).
30. L. Jiang, P. Berraondo, D. Jericó, L. T. Guey, A. Sampedro, A. Frassetto, K. E. Benenato, K. Burke, E. Santamaría, M. Alegre, Á. Pejenaute, M. Kalariya, W. Butcher, J.-S. Park, X. Zhu, S. Sabnis, E. S. Kumarasinghe, T. Salerno, M. Kenney, C. M. Lukacs, M. A. Ávila, P. G. V. Martini, A. Fontanellas, Systemic messenger RNA as an etiological treatment for acute intermittent porphyria. *Nat. Med.* **24**, 1899–1909 (2018).
31. Q. Cheng, T. Wei, Y. Jia, L. Farbiak, K. Zhou, S. Zhang, Y. Wei, H. Zhu, D. J. Siegwart, Dendrimer-based lipid nanoparticles deliver therapeutic FAH mRNA to normalize liver function and extend survival in a mouse model of hepatorenal tyrosinemia type I. *Adv. Mater.* **30**, e1805308 (2018).
32. L. Miao, L. Li, Y. Huang, D. Delcassian, J. Chahal, J. Han, Y. Shi, K. Sadtler, W. Gao, J. Lin, J. C. Doloff, R. Langer, D. G. Anderson, Delivery of mRNA vaccines with heterocyclic lipids increases anti-tumor efficacy by STING-mediated immune cell activation. *Nat. Biotechnol.* **37**, 1174–1185 (2019).
33. J. D. Finn, A. R. Smith, M. C. Patel, L. Shaw, M. R. Youniss, J. van Heteren, T. Dirstine, C. Ciullo, R. Lescarbeau, J. Seitzer, R. R. Shah, A. Shah, D. Ling, J. Growe, M. Pink, E. Rohde, K. M. Wood, W. E. Salomon, W. F. Harrington, C. Dombrowski, W. R. Strapps, Y. Chang, D. V. Morrissey, A single administration of CRISPR/Cas9 lipid nanoparticles achieves robust and persistent in vivo genome editing. *Cell Rep.* **22**, 2227–2235 (2018).
34. C. Jiang, M. Mei, B. Li, X. Zhu, W. Zu, Y. Tian, Q. Wang, Y. Guo, Y. Dong, X. Tan, A non-viral CRISPR/Cas9 delivery system for therapeutically targeting HBV DNA and *pcsk9* in vivo. *Cell Res.* **27**, 440–443 (2017).
35. D. E. Sabatino, T. C. Nichols, E. Merricks, D. A. Bellinger, R. W. Herzog, P. E. Monahan, Animal models of hemophilia. *Prog. Mol. Biol. Transl. Sci.* **105**, 151–209 (2012).
36. A. M. Lange, E. S. Altynova, G. N. Nguyen, D. E. Sabatino, Overexpression of factor VIII after AAV delivery is transiently associated with cellular stress in hemophilia A mice. *Mol. Ther. Methods Clin. Dev.* **3**, 16064 (2016).
37. J. I. Siner, N. P. Iacobelli, D. E. Sabatino, L. Ivanciu, S. Zhou, M. Poncz, R. M. Camire, V. R. Arruda, Minimal modification in the factor VIII B-domain sequence ameliorates the murine hemophilia A phenotype. *Blood* **121**, 4396–4403 (2013).
38. X. Hou, X. Zhang, W. Zhao, C. Zeng, B. Deng, D. W. McComb, S. Du, C. Zhang, W. Li, Y. Dong, Vitamin lipid nanoparticles enable adoptive macrophage transfer for the treatment of multidrug-resistant bacterial sepsis. *Nat. Nanotechnol.* **15**, 41–46 (2020).
39. G. N. Nguyen, L. A. George, J. I. Siner, R. J. Davidson, C. B. Zander, X. L. Zheng, V. R. Arruda, R. M. Camire, D. E. Sabatino, Novel factor VIII variants with a modified furin cleavage site improve the efficacy of gene therapy for hemophilia A. *J. Thromb. Haemost.* **15**, 110–121 (2017).
40. S. I. Chavin, Factor VIII: Structure and function in blood clotting. *Am. J. Hematol.* **16**, 297–306 (1984).
41. M. Rajabi, M. Lanfranchi, F. Campo, L. Panza, Synthesis of a series of hydroxycarboxylic acids as standards for oxidation of nonanoic acid. *Synth. Commun.* **44**, 1149–1154 (2014).
42. X. Zhang, B. Li, X. Luo, W. Zhao, J. Jiang, C. Zhang, M. Gao, X. Chen, Y. Dong, Biodegradable amino-ester nanomaterials for Cas9 mRNA delivery in vitro and in vivo. *ACS Appl. Mater. Interfaces* **9**, 25481–25487 (2017).

Acknowledgments: We acknowledge the use of the core facility provided by the CPMPSR, Campus Microscopy and Imaging Facility (CMIF), and Small Animal Imaging Core (SAIC) at The Ohio State University. **Funding:** Y.D. acknowledges the support from the Maximizing Investigators' Research Award R35GM119679 from the National Institute of General Medical Sciences, R01HL136652 from the National Heart, Lung, and Blood Institute as well as the start-up fund from the College of Pharmacy at The Ohio State University. W.Z. acknowledges the support from the Professor Sylvan G. Frank Graduate Fellowship. **Author contributions:** X.Z. and W.Z. conceived and designed the experiments. X.Z. and W.Z. performed the experiments and wrote the paper. G.N.N. and D.E.S. contributed to the FVIII-related animal study. C.Zh. and W.L. contributed to the in vivo biodegradability study. J.Y. contributed to the confocal microscope imaging. S.D. and X.H. contributed to the flow cytometry assays. C.Ze. and J.Y. prepared the mRNA. J.J. contributed to the chemical synthesis. B.D. and D.W.M. contributed to the cryo-TEM imaging. R.D., A.S., L.B., F.G., M.S., and D.C. contributed to the base editing animal study. D.E.S. and Y.D. conceived and supervised the project and wrote the paper. The final manuscript was edited and approved by all authors. **Competing interests:**

R. D., A. S., L.B., F.G., M. S., and D. C. are employees of Beam Therapeutics. X.Z. and Y.D. are inventors on patent applications filed by The Ohio State University related to the functionalized LLNs in this work. (publication number: WO2019/099501 A1; publication date: 23 May 2019). The authors declare that they have no other competing interests. **Data and materials availability:** The functionalized LLNs can be provided by Y.D. pending scientific review and a completed material transfer agreement. Requests for the functionalized LLNs should be submitted to Y.D. All data needed to evaluate the conclusions in the paper are present in the paper and/or the Supplementary Materials. Additional data related to this paper may be requested from the authors.

Submitted 14 April 2020
Accepted 9 July 2020
Published 21 August 2020
10.1126/sciadv.abc2315

Citation: X. Zhang, W. Zhao, G. N. Nguyen, C. Zhang, C. Zeng, J. Yan, S. Du, X. Hou, W. Li, J. Jiang, B. Deng, D. W. McComb, R. Dorkin, A. Shah, L. Barrera, F. Gregoire, M. Singh, D. Chen, D. E. Sabatino, Y. Dong, Functionalized lipid-like nanoparticles for in vivo mRNA delivery and base editing. *Sci. Adv.* **6**, eabc2315 (2020).